LINEAR CHARGED-PARTICLE ACCELERATORS

OPPORTUNITIES FOR THE USE OF THE SMALL-SIZE ACCELERATOR VGIK-1

D.V. Vinnikiov, I.V. Buravilov, V.B. Yuferov, A.N. Ponomarev, V.I. Tkachev
National Science Center "Kharkov Institute of Physics and Technology", Kharkiv, Ukraine
E-mail: vinniden@gmail.com

The experimental data on modification of the surface of metals, alloys and materials coated using the method of irradiation by a heavy-current electron beam with the energy of 300 keV have been given. The specimen surface structure was studied before and after the irradiation using the method of optic microscopy and the surface layer microhardness measurement. The method of electron microscopy was used to analyze the structure and the sizes of dispersed anode material. The films consisting of the crystals with the size of 6 to 8 nm were obtained. The mass transfer processes that occur in the material of metal targets made of Cu, Ti, Mo, Al were studied. The spatial map was compiled for the X-ray field of the plant. The experiments were carried out to define the action of X-ray radiation on the different types of conditionally pathogenic microflora, in particular such bacteria as Escherichia coli, Staphylococcus aureus, and Bacillus subtilis. The fields of application of the plant were defined.

PACS: 52.80.Vp

INTRODUCTION

The operation and some fields of application of the small-size accelerator (SSA) VGIK-1 were described earlier in scientific papers [1 - 4]. The general view of SSA VGIK-1 is presented on Fig. 1.

Fig. 1. Small-size accelerator VGIK-1. General view

The accelerating technique is continuously improved in order to modify already available properties and also to create some new unique properties of the materials [5]. The action of the beams of charged particles allows us to change such operating characteristics as hardness, wear resistance, fatigue strength, the corrosion and erosion resistance and their improvement results in an increased reliability and service life of the parts and instruments operating in difficult conditions. The structure-&-phase transformations that provide a change in the properties of hard materials are defined by the type and the parameters of particle beams and the initial characteristics of the target substance. By managing their combinations we can provide a wanted change in their properties [6 - 8]. It should be noted that nanomaterial-based technologies are widely used and are very promising. The main branches that demand nanotechnologies are power engineering, electronics, biology and medicine [9]. The irradiation of targets by particle beams with preset parameters enables the dispersion of the material and the formation of the film of an appropriate size and composition. The X-ray radiation generated by the action of high-energy particles on the target material can be used for the irradiation of animate objects in order to have influence on their biological activity [10]. The purpose of this research was to define the opportunities of the SSA VGIK-1 for the solution of different research and technological problems.

1. ACCELERATOR PARAMETERS

The experimental part of this research was carried out using the SSA VGIK-1. Fig. 2 gives the schematic diagram of the plant.

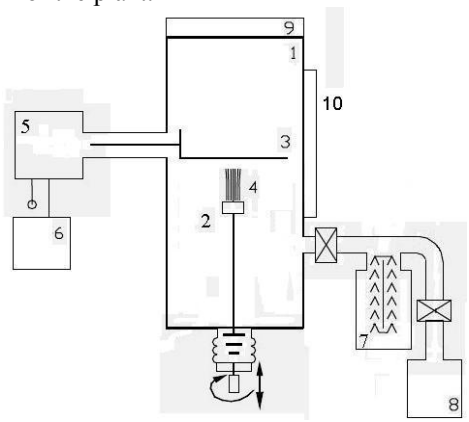

Fig. 2. The schematic diagram of the plant VGIK-1: 1 – vacuum chamber; 2 – emitting electrode; 3 – target electrode; 4 – electron beam; 5 – Max generator; 6 – control unit; 7, 8 – diffusion and high-pressure vacuum pumps; 9, 10 – upper and lateral flanges made of polymethylmethacrylates

The accelerator electrode system consists of the semisphere – the electron emitter, the anode plate whose material was sputtered and deposited on the KCl salt crystal as it shown on Fig. 3.

The interelectrode spacing was controlled in the range of 1…3 cm. The electron beam diameter corresponds to the cathode diameter and it is also confirmed by the imprint on the anode. Hence, the area of the surface modified by the beam is varied in the range of 7…64 cm^2 and it depends on the beam energy, the interelectrode spacing and the target material. Using the test tools we obtained some plant parameters.

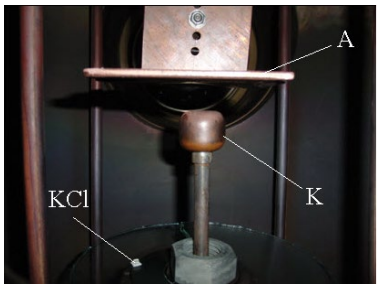

Fig. 3. A general view of the diode system. K is the graphite cathode, A is the anode target, KCl is the test potassium chloride crystal onto which the film was deposited

The structure and the dimensions of deposited material were analyzed using the transmission electron microscope (TEM). The morphology of irradiated surfaces was defined using the optic microscope Olympus GX 51. The processes initiated by the passing beam were recorded by the high-speed video camera Casio Exilim EX-FH100 with the resolution of 1000 shots/s. The current was measured using the Rogowski loop with the sensitivity of 1.96 kA/V. The Vickers microhardness was measured by the microhardness meter PMT-3. The load weight was 50 g. The X-ray dose was measured by radiation receivers. The film morphology of sputtered anode material was defined using the microdiffraction method. The Laue method was used to get the diffraction image of the stationary monocrystal. Such materials as Cu, Ti, Mo, Al and stainless steel were used as the target electrode. The target mass was weighted using the scales of a VLP-200 type with the balance error of 0.5 mg for the specimen of up to 50 g and in the weight range of 50 to 200 g this error was 1 mg. The bacteriological investigations of the survival of conditionally pathogenic microflora were carried out.

The current oscillogram was obtained that allowed us to evaluate the discharge circuit parameters given in the Table 1.

Table 1

SSA parameters, VGIK-1

Charge voltage	Up to 30 kV
Discharge current	Up to 20 kA
Channel resistance	Up to 1.5 Ω
Discharge duration	Up to 5 μs
Circuit induction	9 μH
The number of charge stages	9
Capacitor type	PC-100/0.4
Interelectrode spacing	5…20 mm
Beam energy	250…300 keV
Energy per 1 μs	100 J
Vacuum	$2.5 \cdot 10^{-5}$ Torr

The discharge has an oscillating character and the largest portion of energy is released during one period.

The analysis of the oscillogram and high-speed video-filming data that are given on Figs. 4, 5, allows us to state that the material treatment process is defined not only by the action of the beam but also by the action of plasma in the form of arc.

The accelerator energy was defined experimentally based on the available parameters of the generator of pulsed voltages, in particular the battery capacitance, induction, charge voltage, the electrode material and geometry and also the interelectrode spacing, vacuum conditions and obtained current oscillograms.

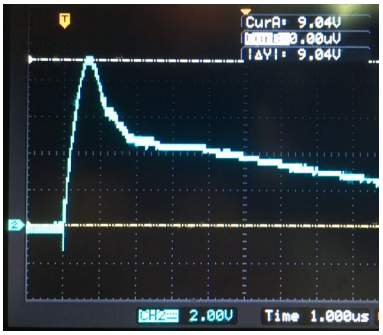

Fig. 4. The current oscillogram

Fig. 5. The high-speed video filming of the discharge at the completion stage

2. EXPERIMENTAL DATA

2.1. MASS TRANSFER

Consideration was given to the processes related to the target material evaporation when exposed to the beam action using the experimental data obtained for the stored energy of 1.5 kJ and the thirty pulses for each specimen.

The computations done using the experimental data given in the Table 2.

Table 2

Mass loss. General data

Target material	Cu	Ti	Mo	Al
Mass M_0, g	61.486	35.405	20.705	17.554
Mass M_1, g	61.007	35.332	20.697	17.430
Mass loss per 30 pulse, mg	478.7	72.9	7.7	123.6
Mass loss per pulse, mg	15.6	2.43	0.25	4.12
Sublimation energy, kJ/g	4.75	9.86	8.7	6.78
Evaporation heat, kJ/g	4.79	8.83	6.15	10.5
Atom mass, 10^{-23} g	10	8	15.9	4.48
The number of atoms removed from the target per 1 pulse, 10^{19} particles	9.69	9.2	0.15	3.05
The minimum energy input for the sublimation of the lost mass, J	48.55	23.95	1.7	35.8
Energy falling to one atom per pulse, eV	3.13	4.89	6.77	2.42

The Table shows that the highest mass loss is observed for the materials with the lowest sublimation energy, i.e. copper and aluminum. At the same time, the evaporation heat of copper is 1.3 to 2 times higher than that of other materials in question and it also conditions the more intensive mass transfer. The material evaporation is also possible for Ti, Mo, Al targets with its transfer to the gaseous phase, because input energies exceed those required for the transfer to the gaseous phase. The molybdenum specimen is evaporated with a considerably lower intensity, i.e. 10 times slower than titanium and 62 times slower than copper due to high values of the sublimation energy and atomic weight.

Fig. 6 gives a general view of the specimens before and after the treatment at a 40-fold magnification.

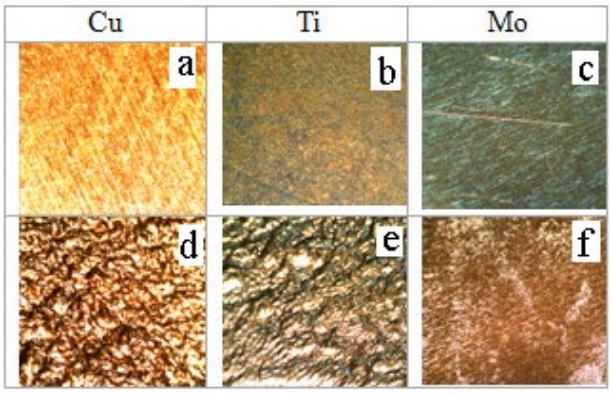

Fig. 6. The microstructure of the surface irradiated by electron beams with the energy of 300 keV for Cu, Ti, Mo. a, b, c – before the irradiation; d, e, f – after the irradiation

It can be seen that the mass loss results in the surface modification of all the specimens.

2.2. SURFACE MODIFICATION

During the interaction of the heavy-current electron beams with the solid body surface we observe the set of processes that represent the common phenomenon and are called the ablative interaction. The ablation is characterized by many processes that occur simultaneously, in particular heating, melting and evaporation of the entire area or just a portion of the interaction area, the plasma torch formation, the plasma outflow and the neutral gas emission from the interaction area, the so-called discharge and the formation of shock waves in the solid body.

The technical use of the ablation process for the modification of the surface structure of metals that provides an increased strength and corrosion resistance requires as a rule no evaporation of a large amount of the material; it is sufficient to bring the surface to melting with the subsequent fast cooling of the target retaining thus the melted material structure. The surface evaporation is also reasonable for the removal of low-energy admixtures. The main contribution to the modification of the structure of internal areas is made by the shock wave that is propagated in the solid body from the ablation zone.

Fig. 7 gives the specimens made of copper and stainless steel. Figs. 7; 8,b depict the marked zones that differ from each other by the degree of a change in the morphology of surface layers and these are given in detail in Figs. 7; 8,c.

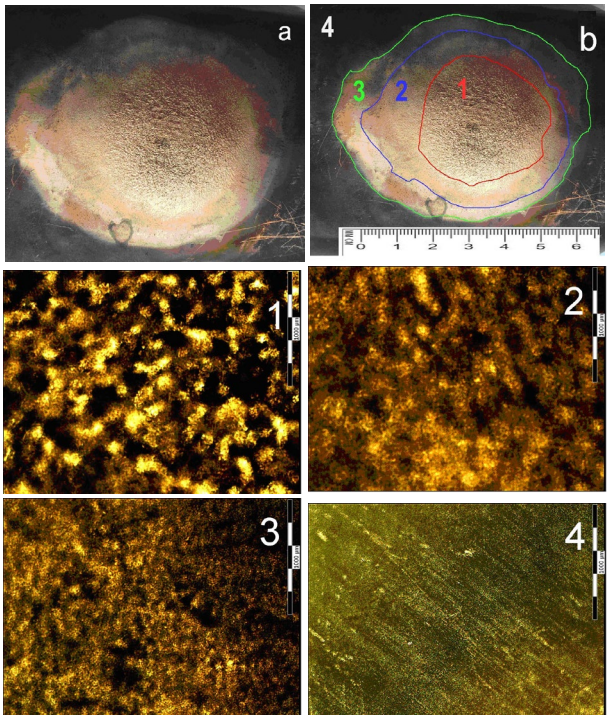

Fig. 7. Copper surface morphology after the plasma beam treatment, a – general view of the specimen treated using the plasma beam method; b – specimen with marked characteristic zones; 1, 2, 3, 4 – view of zones with a 50-fold magnification

Fig. 7,a gives the specimen subjected to the plasma beam treatment with no marked zones. The 4th zone corresponds to the reference specimen that was not subjected to the plasma beam treatment.

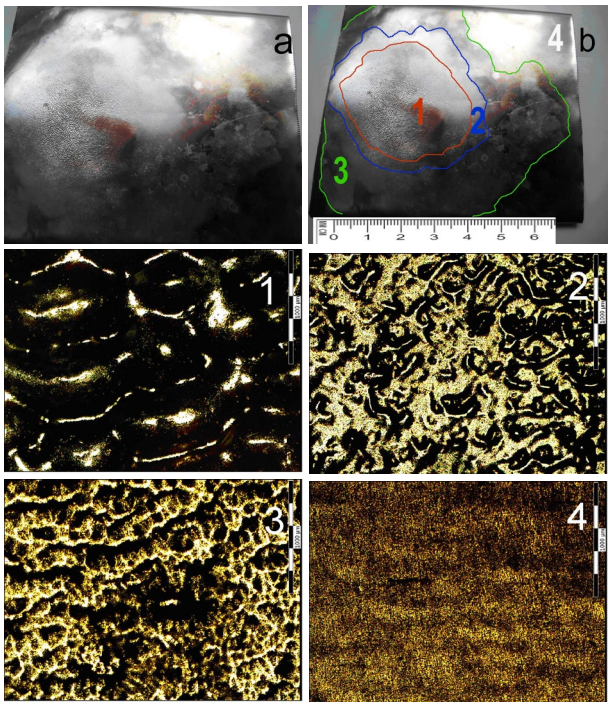

Fig. 8. Stainless steel surface morphology after the plasma beam treatment, a is a general view of the specimen treated using the plasma beam method; b – specimen with marked typical zones; c:1, 2, 3, 4 – view of the zones with a 50-fold magnification

A difference in the surface of different materials after their treatment depends on their physical properties (heat conductivity, vapor tension, mechanical properties, etc) and the composition. The zones with intensive heating show the sublimation temperature inhomogeneity. The copper is represented in its pure form. The shape of bright formations is very close to spherical and these formations have no great amount of dark spots and are distributed uniformly across the entire surface. It is peculiar for all the three zones exposed to the treatment, including the first zone where the heating is the most intensive. Such morphology can be indicative of the availability of a great amount of admixtures and it is conditioned first of all by the presence of contaminants on the material surface and approximately identical evaporation rates.

For stainless steel the evaporation of contained admixtures is defined by the vapor tension of each element. Cr whose content varies from 12 to 20% is evaporated first. We can see typical ripples in the domain № 1 with prevailing dark areas and it is indicative of the possible evaporation of a number of alloying elements. Stainless steel contains the elements that are associated with iron and its alloys (C, Si, Mn, S, P). Many alloying elements Ni, Mn and Ti, Nb, Co, Mo are present here, therefore the surface is sublimated non-uniformly and each element has the melting temperature and the evaporation temperature of its own. Its vapor tension is high and it starts to evaporate already at 1100ºC.

The availability of different zones is also explained by the nonuniform electron beam energy release in the material. The microhardness measurement data taken across the thickness of irradiated plate are indicative of the fact that the microhardness level is 1.8 to 2.2 times higher in the zone of the most intensive heating, i.e. zone № 1 in comparison with the average value of the target microhardness before the treatment. Hence, we can speak of the available effect produced by the action of the pulsed plasma beam on the surface structure of studied targets.

2.3. THE IRRADIATION OF COATED SPECIMENS USING THE PLASMA-ARC METHOD

The studies of the processes that occur during the interaction of the beams of charged particles and plasma both with the surfaces of pure materials and those with already applied coatings are of great importance for the development of technologies related to the use of materials with new properties. Consideration was given to the opportunity of a change in the properties (in particular microhardness) of the materials that were coated using the plasma – arc method and the Bulat-6 plant. Fig. 9 gives appropriate specimens before and after the irradiation using the SSA plant VGIK-1.

Fig. 9. The surface morphology of the specimens that were coated using the Bulat-6 plant after the irradiation by the SSA plant VGIK-1

Table 3 gives microhardness measurement data for the series of specimens before and after their irradiation.

Table 3

Microhardness measurement data

Mat.	Iarc, A	Hititial, HV	Hirrad, HV	PMT-3
Cu/ NbN	80 100	473	501	50 g 5·5 mm^2
Cu/ NbN	80 85	358	701	
Cu/ Zr	80 90	501	739	
Cu/ Nb	80 105	332	435	
CuN/ CrN	85 80	236	251	
CuN/ CrN	85 80	453	701	
ZrN/ CuN	85 80	401	891	
TiZrN/ TiSiN	85 80	787	418	

It can be seen that approximately two-times increase in the hardness is peculiar for irradiated materials depending on the specimen composition.

2.4. FILM DEPOSITION

The target material surface modification process is accompanied by its dispersion. Fig. 10 gives the film formed by the sputtered material on the cathode and the target electrode surface after thirty pulses.

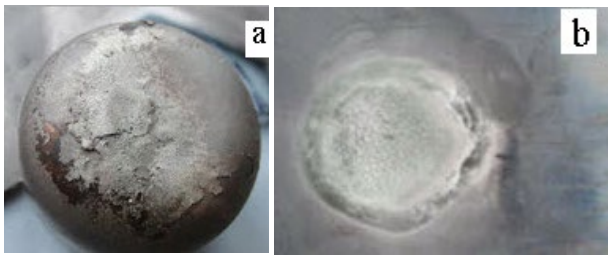

Fig. 10. The deposition on the cathode (a) and the Ti target surface irradiated with the electron beams of 270 keV (b)

The structure and the dimensions of deposited material were analyzed using the transmission electron microscope (TEM). The measurements were taken for the electron energy of 125 kV in the bright field with the marked region diffraction (SAED). All the images were obtained for film ruptures or for the places transparent for the electrons. It was established that the film is continuous and inhomogeneous; the drop fraction can be seen. Thin layers show that the film is fine-crystalline. We can state that the film is multilayered. The film morphology consists of almost continuous coating that contains the agglomerates with the size of 50 to 100 nm; the entire field of the film contains small crystals with the size of 6 to 8 nm. The agglomerates can consist of the same nanocrystals or the phase that forms a continuous film coating.

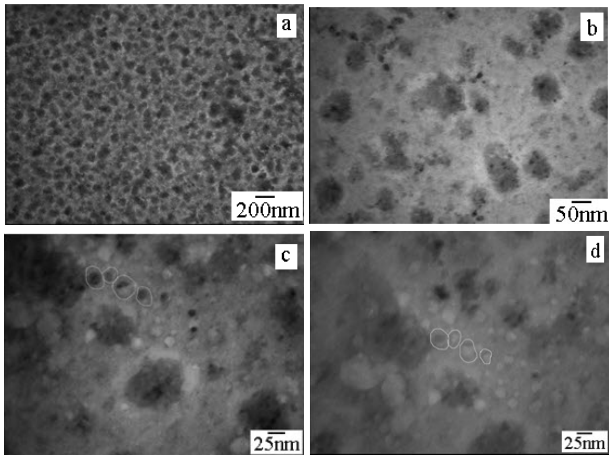

Fig. 11. A typical structure of the material deposited on the KCl crystal surface. Magnification by 10^4 (a), $4 \cdot 10^4$ (b), $8 \cdot 10^4$ (c, d)

The nanocrystal evaporation phenomenon was observed for the electron beam action. Fig. 11,c shows the same zones at the beginning of filming and Fig. 11,d shows them after the exposure to the electron beam during several minutes. Hence, all the bright spots on the images with the 80000-fold magnification are the result of the evaporation of nanocrystals under the action of electron beam.

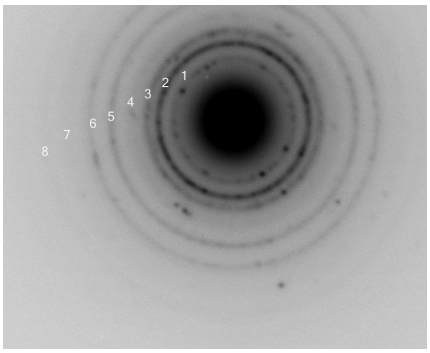

Fig. 12. The Lauegram (250000-fold magnification) of copper deposited on the KCl crystal surface

The method of microdiffraction was used to obtain the Lauegram (X-ray pattern) shown in Fig. 12, where the narrow X-ray beam of a continuous spectrum was directed at the stationary monocrystal that represents the X-rays diffraction lattice. The diffraction pattern created by the crystal was registered by the photographic film placed behind the crystal. In addition to the central spot formed by the undeflected X-ray beam the Lauegram shows the ring spots whose number and location depend on the type of crystal and its orientation relative to the beam. We detected nine ring spots on the Fig. 12. Hence, we can draw a conclusion that the film has the crystalline structure.

The analogous data were obtained for other target materials. The multilayered films that contain the nanosize crystals of the anode material were thus obtained on the cathode.

2.5. X-RAY RADIATION TOPOGRAPHY

To define the X-ray radiation action opportunities of the tested accelerator with regard to the materials and objects its spatial map was made and shown on Fig. 13.

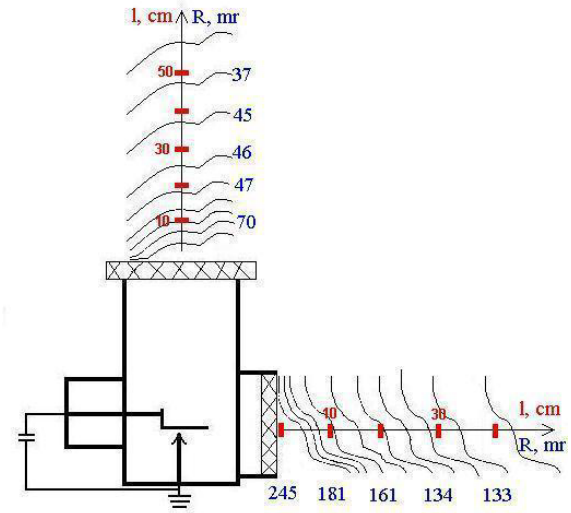

Fig. 13. X-ray radiation topography near lateral and upper flanges. Side view

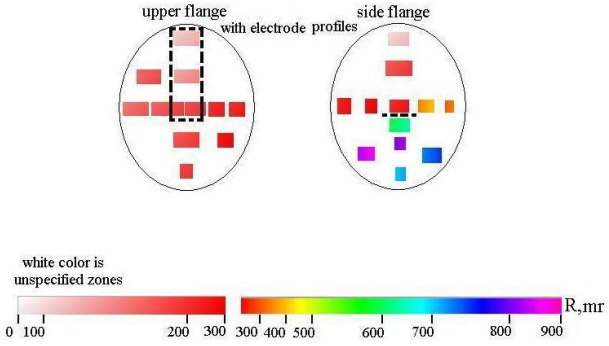

Fig. 14. The color map of the X-ray intensity on the surface of lateral and upper flanges

The X-ray sensors were placed across the area of each flange and also lengthwise at a distance of up to 50 cm from the flanges. Fig. 14 shows the measurement data that allowed us to establish that the radiation is more intensive near the lateral flange where the total dose after the 10 pulses is equal to 245 mR, and for the upper flange it is equal to 100 mR.

The obtained data enabled the establishment of the zones of the most intensive radiation. The regions that are the most convenient for the placement of treated materials beyond the accelerator chamber have been defined.

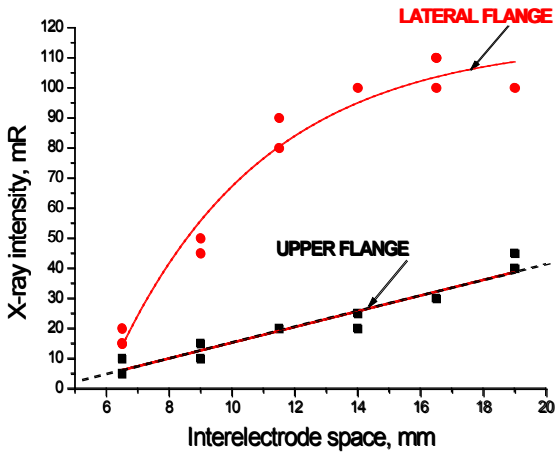

Fig. 15. Dependence of the X-ray intensity on the interelectrode spacing

The dependence of the X-ray intensity on the interelectrode spacing was defined as it shown on Fig. 15. The spacing control unit structure does not permit to increase the gap by more than 20 mm.

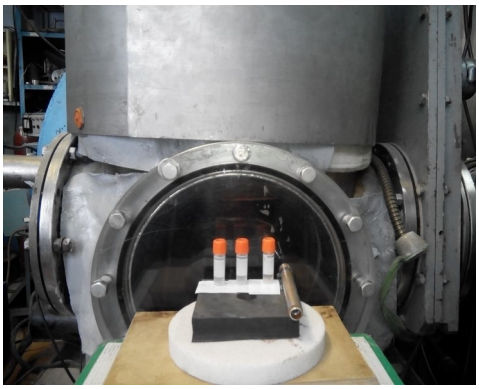

Fig. 16. Conditionally pathogenic microflora irradiation

Preliminary experiments were carried out to define the X-ray influence on different types of conditionally pathogenic microflora, in particular the bacteria of Escherichia coli, Staphylococcus aureus, Bacillus subtilis types. The general view of experiment is shown on Fig. 16. The methods and the conditions required for the realization of mutational, bactericidal and bacteriostatic effects onto the bioobjects have been defined.

CONCLUSIONS

The experiments carried out allowed us to define the methods of the development of the SSA VGIK-1. At the moment, we can mark out the following lines:

- Changing the material surface microhardness;
- Hardening copper-containing material surfaces;
- Applying the films consisting of nanocrystals onto the substrates;
- Using the plant as an X-ray source with the doses of up to ~100 mR/pulse and with the accumulated doses of up to ~ 2000 mR/h at the pulse repetition rate of 3 pulses per minute.

It should be noted in conclusion that some energy and technology characteristics of the small-size accelerator – VGIK-1 were defined. The plant was used to do research in order to increase the surface microhardness of metals, alloys and the materials with the preliminary applied coatings including those made of nitrides. Cu, Ti, Al, and stainless steel specimens were subjected to the irradiation. The morphology of irradiated specimens made of Cu, Ti, and stainless steel was defined. The X-ray field map was compiled. An optimal interelectrode spacing was defined to get maximum X-ray doses.

The investigation was carried out in cooperation with the Institute for the Solid – State Physics. Material Science and Technologies of the National Academy of Sciences of Ukraine (NASU) to treat a series of multicomponent specimens with the coatings applied using the plasma-arc method. The morphology of the anode material sputtered on the KCl crystal was defined in cooperation with the Institute of Single Crystals of the NASU. The conditionally pathogenic flora was treated in cooperation with the Institute of Cryobiology and Cryomedicine of NASU.

The accelerator with electron beam parameters (the electron energy of up to 270 keV, the pulse duration of up to 5 μs, and the pulse frequency of 20 pulse/h) can be recommended for the purposeful surface modification of the metals, alloys and materials with applied coatings used for different research and technological purposes and also for the investigation of the X-ray effect on different microflora for medical purposes.

REFERENCES

1. G.A. Mesyatz, D.I. Proskurovskiy, V.P. Rotshtein, N.I. Lebedeva. Low-Energy Pulsed Electron Beam of a High Density for the Surface Heating // *DAN USSR*. 1983, v. 253, № 6, p. 1383-1386.
2. V.B. Yuferov, E.I. Skibenko, L.G. Sorokovoy, et al. On the Possibility of the Use of the System of Pulsed Electron Accelerator to Modify the Surface-Volumetric Properties of Different Materials // *Problems of Nuclear Science and Engineering. Series "The Physics of Radiation Damages and the Radiation Material Science"*. 1997, Issue 1(66), 2(66), p. 197-198.
3. V.F. Zelenskiy, I.M. Neklyudov, V.F. Rybalko, S.V. Shevchenko, et al. *Influence of the Irradiation by Pulsed Plasma Streams on the Mechanical Properties of Austenitic Stainless Steel X16H15M3B and X18H10T*: preprint KhFTI 89-64, Kharkov, 1989, 12 p.
4. V.B. Yuferov, L.G. Sorokovoy, E.I. Skibenko, Yu.V. Holod, E.V. Mufel. Some Applications of High-Voltage High-Power Pulsed Equipment // *Problems of Atomic Science and Technology. Series "Vacuum, Pure Materials and Superconductors"*. 1999, Issue 2 (10), p. 21-25.
5. A.N. Dovbnya, V.V. Zakutin, A.A. Parhomenko, O.A. Repihov, N.G. Reshetnyak, et al. Electron Beams for Radiation Technologies // *Problems of Atomic Science and Technology. Series "Physics of Radiation Effect and Radiation Materials Science"*. 2002, № 6, p. 152-153.
6. A.N. Dovbnya, S.D. Lavrinenko, V.V. Zakutin, A.N. Aksenova, N.G. Reshetnyak, N.N. Pilipenko, V.N. Pelyh, G.N. Tolmacheva. The Zirconium and the Zr1%Nb Alloy Surface Modification by the Electron Beam of the Magnetron Gun-Based Accelerator // *Problems of Atomic Science and Technology. Series "Physics of Radiation Effect and Radiation Materials Science"*. 2011, № 2, p. 39-45.
7. A.D. Pogrebnyak, O.P. Kulmentieva. Structure and Phase Transformations in the Surface Layers and the Properties of Metal Materials after the Pulsed Action of Particle Beams // *PSE*. 2003, Issue 1, № 2, v. 1.
8. A.B. Batrakov, M.I. Bazaleev, S.E. Donets, V.F. Klepikov, Yu.F. Lonin, V.V. Lytvynenko, A.G. Ponomarev, V.V. Uvarov, V.T. Uvarov, V.N. Robuk. The Particularities of the Influence Produced by High-Current Relativistic Electron Beams on Construction Material Targets // *Problems of Atomic Science and Technology. "Nuclear Physics Investigations"*. 2013, № 6, p. 225-229.
9. A.P. Chernyaev, M.A. Kolyvanova, P.Yu. Borshegovskaya. Radiation Technologies in Medicine. Part 1. Medical Accelerators. Biophysics

and Medical Physics. Seria 3 // *Phisics. Astronomy*. 2015, № 6, p. 28-36.
10. A.A. Tsutsaeva, I.P. Vysekancev, N.F. Severin, Yu.A. Itkin. Lethal and Mutagenic Action of the Electron Irradiation on the *r* II Mutant Phage T4 in the Low-Temperature Range (-196ºC) // *Radiobiology*. 1981, v. 21, p. 133-134.

Article received 05.11.2019

ВОЗМОЖНОСТИ ИСПОЛЬЗОВАНИЯ МАЛОГАБАРИТНОГО УСКОРИТЕЛЯ ВГИК-1

Д.В. Винников, И.В. Буравилов, В.Б. Юферов, А.Н. Пономарев, В.И. Ткачев

Представлены экспериментальные результаты по модифицированию поверхности металлов, сплавов и материалов с нанесенными покрытиями методом облучения сильноточным электронным пучком с энергией до 300 кэВ. Изучены структура поверхности образцов до и после облучения методом оптической микроскопии и измерения микротвердости в поверхностном слое. Методом электронной микроскопии проведен анализ структуры и размеров распыляемого материала анода. Получены пленки, состоящие из кристаллов с размером 6…8 нм. Исследованы процессы массопереноса материала металлических мишеней Cu, Ti, Mo, Al. Составлена объемная карта рентгеновского поля установки. Проведены эксперименты по воздействию рентгеновского излучения на различные типы условно патогенной микрофлоры: бактерии типа Escherichia coli, Staphylococcus aureus, Bacillus subtilis. Определены дальнейшие направления применения установки.

МОЖЛИВОСТІ ВИКОРИСТАННЯ МАЛОГАБАРИТНОГО ПРИСКОРЮВАЧА ВГІК-1

Д.В. Вінніков, І.В. Буравілов, В.Б. Юферов, О.М. Пономарьов, В.І. Ткачов

Представлено експериментальні результати по модифікації поверхні металів, сплавів і матеріалів з нанесеними покриттями методом опромінення потужнострумовим електронним пучком з енергією до 300 кеВ. Вивчена структура поверхні зразків до і після опромінення методом оптичної мікроскопії та вимірювання мікротвердості в поверхневому шарі. Методом електронної мікроскопії проведено аналіз структури і розмірів розпорошуваного матеріалу анода. Отримано плівки, що складаються з кристалів розміром 6…8 нм. Досліджено процеси масопереносу матеріалу металевих мішеней Cu, Ti, Mo, Al. Складено об'ємну карту рентгенівського поля установки. Проведено експерименти з впливу рентгенівського випромінювання на різні типи умовно патогенної мікрофлори: бактерії типу Escherichia coli, Staphylococcus aureus, Bacillus subtilis. Визначено подальші напрямки застосування установки.